http://dx.doi.org/10.5012/bkcs.2014.35.11.3143

Accounts

The Electrochemical Reaction Mechanism and Applications of Quinones

R. Soyoung Kim and Taek Dong Chung*

*Department of Chemistry, Seoul National University, Seoul 151-747, Korea. *E-mail: tdchung@snu.ac.kr*
Received July 8, 2014, Accepted July 23, 2014

This tutorial review provides a general account of the electrochemical behavior of quinones and their various applications. Quinone electrochemistry has been investigated for a long time due to its complexity. A simple point of view is developed that considers the relative stability of the reduced quinone species and the values of the first and second reduction potentials. The 9-membered square scheme in buffered aqueous solutions is explained and semiquinone radical stability is discussed in this context. Quinone redox reaction has also been employed in various studies. Diverse examples are presented under three broad categories defined by the roles of quinone: molecular tool for physical chemistry, versatile electron mediator, and charge storage for energy conversion devices.

Key Words : Quinone electrochemistry, 9-Membered square scheme, Semiquinone radical, Electron mediator, Organic electrode material

Introduction

Quinones are conjugated cyclic diones derived from aromatic compounds[1] that undergo facile two-electron redox reaction. Having moderate reduction potential that can be modulated in a wide range, quinones play important roles in nature (Figure 1). Most importantly, quinone (*e.g.* ubiquinone, plastoquinone) relays electrons in the biological redox machinery for photosynthesis and respiration. As they shuttle electrons along the membrane and repeat reduction and oxidation, they transport protons across the membrane. Quinones and hydroquinones also act as dyes (*e.g.* lawsone), antibiotics (*e.g.* adriamycin, daunorubicin), cofactors (*e.g.* pyrroloquinoline quinone, topaquinone), vitamins (*e.g.* vitamin K's), food and cosmetics additives, and so on. Quinone functionalities are also present in carbon materials after oxidative treatment. Being an electron acceptor, benzoquinone with unsubstituted site easily reacts with nucleophiles. The oxidized form of catechol (1,2-benzoquinone) is more reactive and easily undergoes polymerization at moderate to high pH. The *ortho* configuration of catechols allows them to act as efficient metal chelators and ligands.

Electrochemical methods have proven useful for characterizing the redox reaction of quinones. For more than 100 years, people have studied the reduction and oxidation of various quinone compounds on various electrode materials, in aprotic and aqueous solutions of varying composition. The reviews of Chambers published in 1974 and 1988 are good guides to such research efforts.[2,3] An important aim of electrochemical investigation of quinones is to elucidate their reaction in biological processes. For example, the Q_A site and Q_B site of bacterial photosynthetic reaction center show very different reactivity and a great deal of endeavors are still continuing to fully understand the kind of interactions that lead to such difference.[4] Similarly, the Q cycle in electron transport chain indicates that the electrochemical property of quinones at Q_i and Q_o sites should be carefully tuned in order to suppress reactive oxygen species generation.[5] The mechanism involved in quinone toxicity is also of great interest, which mainly consists of reactive oxygen species generation and reaction with thiol nucleophiles.[6] A recent review shows how drug development can be aided by electrochemical investigations, with a focus on quinone compounds.[7] The studies of quinone electrochemistry also contributed to our understanding of proton-coupled electron transfer (PCET) reactions. A review on electrochemical approach to PCET mechanism devotes a great portion to quinones.[8]

R. Soyoung Kim. (b. 1989) received her B.S. (2012) and M.S. (2014) degrees from the Department of Chemistry at Seoul National University. She is currently a Ph.D. student in the Department of Chemistry at Massachusetts Institute of Technology.

Taek Dong Chung. (b. 1968) received his B.S. (1991), M.S. (1993) and Ph.D.(1997) degrees from the Department of Chemistry at Seoul National University. He worked at California Institute of Technology and Oak Ridge National Laboratory as a postdoc before joining Sungshin Women's University as an assitant professor in 2002. In 2007 he transferred to the Department of Chemistry at Seoul National University as an associate professor and has been serving as a professor since 2012. He won a number of awards including KCS-Wiley young chemist award, Choi Q-Won award, and KCS research excellence grand prize. His research is about fundamental issues on electrochemistry, i.e. electrocatalytic mechanism within confined space, iontronic neuronal interface, suspension array based multiplex analytical system, and new strategies of electrochemical energy conversion.

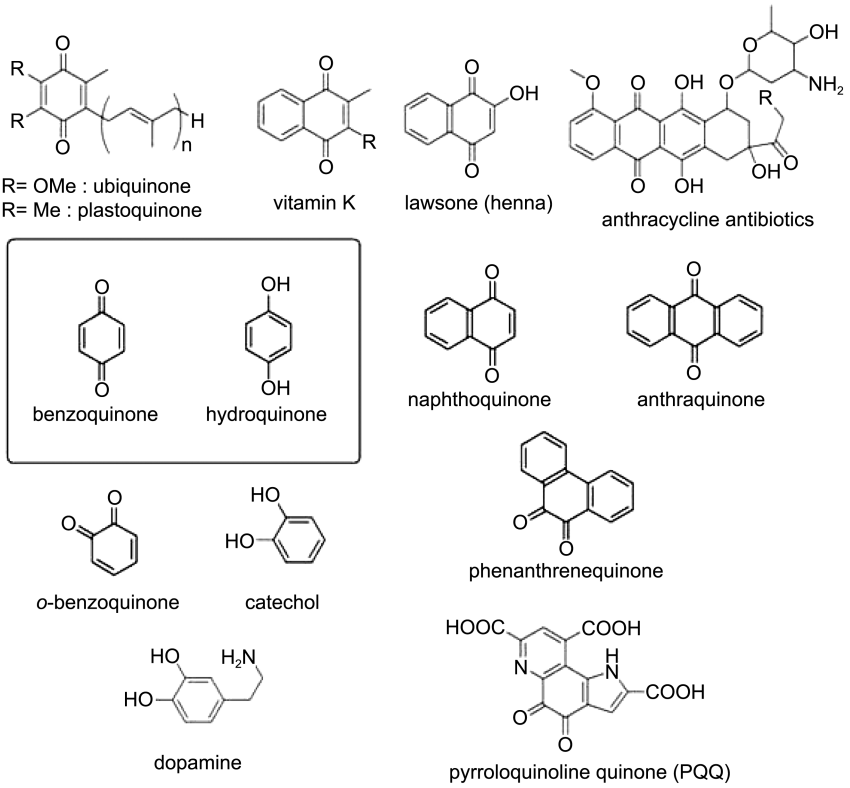

Figure 1. Various quinone and hydroquinone compounds.

The long history of quinone electrochemistry implies not only its importance but also its complexity. Electron transfer to quinones is complicated by dynamic contributions of hydrogen bonding, proton donating and ion pairing effects. Also, quinones undergo inner-sphere electron transfer so that different electrode surfaces give rise to widely different reaction rates. For example, different pretreatment or surface modification of carbon electrode brought about a huge difference in kinetics,[9,10] and adsorption of quinones led to unusual electrochemical behavior.[11,12] Such aspects of quinone electrochemistry will be left out of the scope of this review.

In this tutorial review, we will first summarize the general electrochemical behavior of quinones. Though quinones can show very different voltammetric responses in different solution environments, there are simple principles that can be invoked to understand their behavior. Then the electrochemistry of quinone in buffered aqueous media will be explained based on Laviron's analysis of the "9-membered square scheme," which provides a systematic approach to understand quinone redox reaction. Some examples of mechanism analysis will be presented as well. Meanwhile, with better understanding of the redox reactions of quinones and greater interest in creative research using small organic molecules, various applications using quinones have appeared in the literature. However, as the examples span a wide range of chemical discipline, there are few reviews that focus specifically on quinones. In the second part of this review, we will illustrate some interesting researches that utilized quinone electrochemistry in aqueous media to achieve a variety of purposes.

With the limited space, we do not aim to be comprehensive or in-depth in our presentation. Interested readers will be referred to a number of other review articles. As the figures are adapted from various sources, they may have different convention for the sign of the axes, but a negative sign always indicates reduction.

Understanding the Electrochemistry of Quinones

Aprotic and Unbuffered Aqueous Solutions. It is useful to start the discussion of quinone electrochemistry in aprotic solutions where no hydrogen bonding or proton source is present in principle. It is the simplest case and the quinone undergoes two sequential one-electron reductions, *i.e.* $Q \rightleftarrows Q^{\bullet-} \rightleftarrows Q^{2-}$. Accordingly, two well-separated redox waves can be observed (Figure 2(a)). Extensive tabulation of reduction potential values for various quinones in different solvents and electrolytes are given in a classic review of quinone electrochemistry.[2] Due to the high instability of Q^{2-}, the second reduction peak is sometimes not as well-resolved as the first peak. These voltammetric features are sensitive to hydrogen bonding and protonation that can stabilize the semiquinone radical anion ($Q^{\bullet-}$) and the hydroquinone dianion (Q^{2-}). When hydrogen bond donors such as water or alcohols are added, the redox peaks shift toward positive potential progressively. The redox peak that corresponds to second reduction ($Q^{\bullet-} \rightleftarrows Q^{2-}$) shifts by a larger degree than the redox peak that corresponds to first reduction ($Q \rightleftarrows Q^{\bullet-}$),

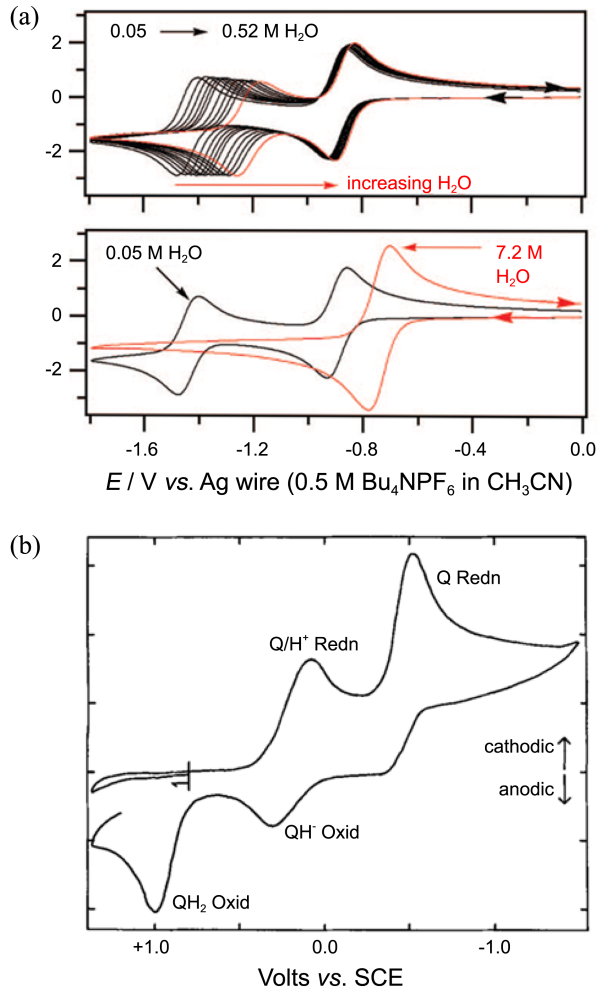

Figure 2. (a) Cyclic voltammograms of vitamin K_1 in 0.2 M Bu_4NPF_6/CH_3CN containing different concentrations of water. Reproduced with permission from ref. 18. © 2009 American Chemical Society. (b) Cyclic voltammogram of 1.52 mM 1,4-benzoquinone in 0.01 M Et_4NClO_4/CH_3CN + 1.91 mM $HClO_4$. Reproduced with permission from ref. 13. © 1970 The Electrochemical Society.

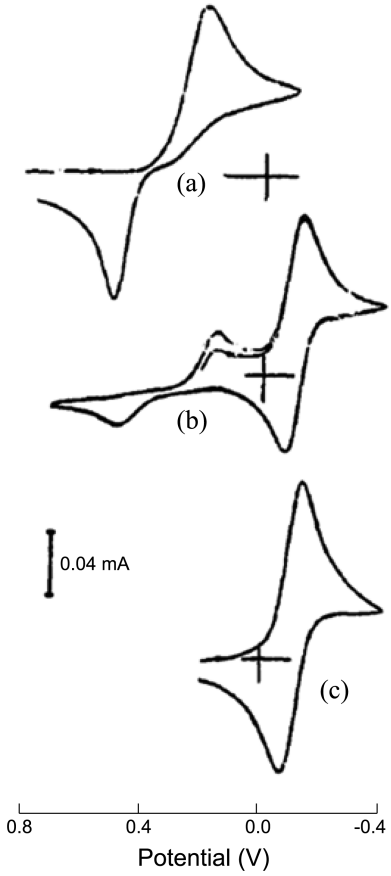

Figure 3. Cyclic voltammograms in unbuffered aqueous solutions of 1.0 mM 1,4-benzoquinone in 1 M KCl at pH: (a) 1.30, (b) 3.11 and (c) 8.83. Reproduced with permission from ref. 20. © 1997 Elsevier.

which indicates that Q^{2-} is stabilized more than $Q^{\bullet-}$ by hydrogen bonding. Eventually the two redox peaks overlap, showing a single redox peak that corresponds to the two-electron reduction of $Q \rightleftarrows Q^{2-}$.

When acids are added as proton donors, distinct peaks appear in the voltammogram rather than a gradual shift of redox potential as with hydrogen bonding (Figure 2(b)). Each peak arises from different protonation states of the quinone species. The effect of hydrogen bonding and protonation on quinone/hydroquinone electrochemistry in aprotic solutions is well studied and reviewed. For example, the effect of different acids and hydrogen bond donors as well as the effect of different substituents,[13,14] estimation of the coordination number of hydrogen bonding agents,[15] comparison of intra- and intermolecular hydrogen bonding[16] have been reviewed. A recent review article covers a large body of literature.[17]

In aqueous solutions, the solvent itself is an excellent hydrogen bonding agent, so that addition of hydrogen bonding donor is meaningless. At pH values where $[H^+] << [Q]$ (Figure 3, curve c), a single redox peak as seen in aprotic solutions with a large amount of hydrogen bonding agent is observed. This corresponds to $Q \rightleftarrows Q^{2-}$, with Q^{2-} being hydrogen bond-stabilized by surrounding water molecules and being at equilibrium with QH^- and QH_2.[19] When $[H^+] >> [Q]$ (Figure 3, curve a), quinone is reduced to hydroquinone QH_2 at a more positive potential since QH_2 is more stable than Q^{2-}. The redox waves with large peak-to-peak separation appear, indicating slow kinetics that will be explained soon. Then, at intermediate pH with $[H^+] \approx [Q]$ (Figure 3, curve b), some of the quinones are reduced to hydroquinone, deplete protons near the electrode surface, and the remaining quinones are reduced to Q^{2-} at a more negative potential, giving rise to two peaks.

The above discussion shows that quinone reduction follows the same principle in aqueous and aprotic solutions, *i.e.* stabilization of the reduced quinone species ($Q^{\bullet-}$ and Q^{2-}) by hydrogen bonding and/or protonation[19]. However, Figures 2 and 3 indicate that quinone electrochemistry can become quite complex in aprotic or unbuffered aqueous solutions. In this regard, buffered aqueous solutions that maintain constant pH provide a convenient platform to study quinone

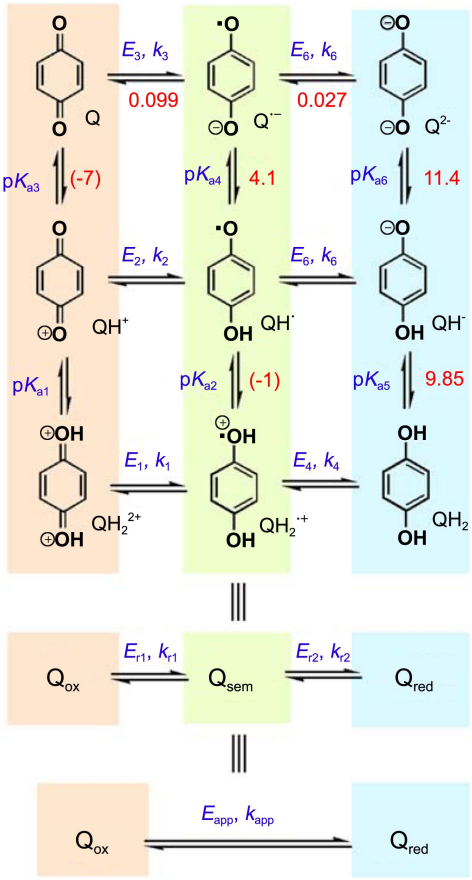

Figure 4. The 9-membered square scheme for quinones. Red numbers represent values for 1,4-benzoquinone.[21] Parentheses indicate rough estimation.

electrochemistry with simplified solvent effects. In fact, even a complete analytical description has been given with some assumptions, as will be presented in the next section.

Buffered Aqueous Solutions: the Square Scheme. In buffered aqueous solutions, quinone shows a single redox peak that corresponds to $Q \rightleftarrows QH_2$ and its reduction potential shows a good linear dependence on pH with a slope of –59 mV/pH, in accordance with the Nernst equation.

$$E = E^0 + \frac{0.0592}{2}\log\frac{[Q][H^+]^2}{[QH_2]}$$

$$= E^0 + \frac{0.0592}{2}\log\frac{[Q]}{[QH_2]} - 0.0592\ \text{pH}$$

At higher pH that exceeds the pK_a of QH_2, the slope decreases to –29 mV/pH and finally to 0 mV/pH, corresponding to the generation of QH^- and Q^{2-}. Although it appears to be simple, the two-electron, two-proton reduction and oxidation of quinone/hydroquinone involves several steps in its detailed mechanism. It can be described by the "9-membered square scheme" (Figure 4). Three protonation states exist for each redox state, and three redox states exist for each protonation state, giving rise to a total of 9 species.

Protonation and deprotonation reactions may be assumed to be at equilibrium, considering the fast diffusion of protons

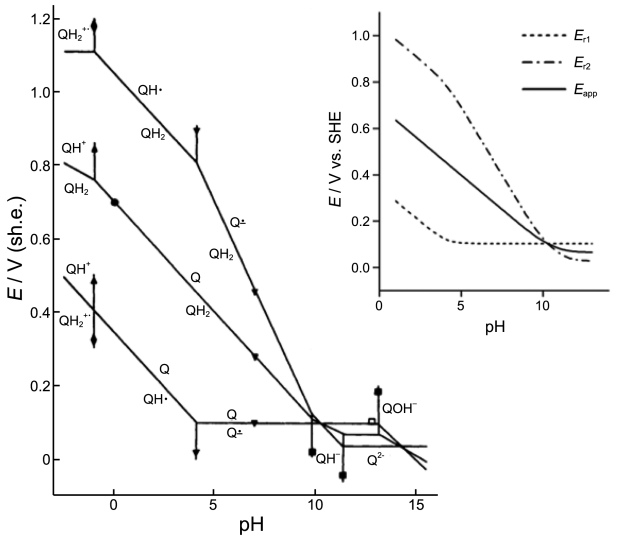

Figure 5. The Pourbaix diagram of 1,4-benzoquinone. Reproduced with permission from ref. 23. © 1983 Royal Society of Chemistry. (Inset) *E*-pH plot showing E_{r1}, E_{r2} and E_{app} only.

and diffusion-controlled rate of protonation reaction.[22] Then the ratio of different protonation states of each redox state will be constant at a given pH, and only electron transfer can be considered to have a kinetic barrier. With this assumption, the two-electron, two-proton reduction and oxidation of quinone can be understood as simple two-electron transfer, grouping the different protonation states together to represent the reaction as $Q_{ox} \rightleftarrows Q_{sem} \rightleftarrows Q_{red}$. The associated E_{ri} and k_{ri} values are functions of pK_{ai}'s and solution pH, of which equations can be found elsewhere.[8,21] The reduction potential and rate constant for the overall redox reaction are designated as E_{app} and k_{app}, and E_{app} is the average of E_{r1} and E_{r2}.

If the individual E_i and pK_{ai} values in the square scheme are known, a Pourbaix diagram that shows the stability of different quinone species at different potential and pH values can be constructed. An example is given for 1,4-benzoquinone (Figure 5). Each line denotes the equilibrium potential for the two redox species marked on it. Because the semiquinone radical is unstable, the zones for Q and QH_2 overlap, and the line in the middle marks the equilibrium potential for Q/QH_2 couple, E_{app}. In the inset of Figure 5, only the values of E_{ri} and E_{app} are shown for clarity.

For many quinone compounds, the reduction potentials and pK_a values in water have been obtained and tabulated.[24,25] It is found that the pK_a values of hydroquinone are much bigger than that of the semiquinone while $E_{Q/Q^{\bullet-}}$ and $E_{Q^{\bullet-}/Q2-}$ are similar; normally the pK_a of $QH^{\bullet}$ is in the range 4-5 while those of QH_2 and QH^- are in the range 9-11. As a consequence, E_{r2} becomes more positive than E_{r1} except at high pH (Figure 5). The situation where the second electron transfer (E_{r2}) is thermodynamically easier than the first (E_{r1}) is called potential inversion. Along with hydrogen bonding of water, such difference in pK_a values and the resulting potential inversion lead to semiquinone being relatively destabilized in aqueous media, so that only a single two-

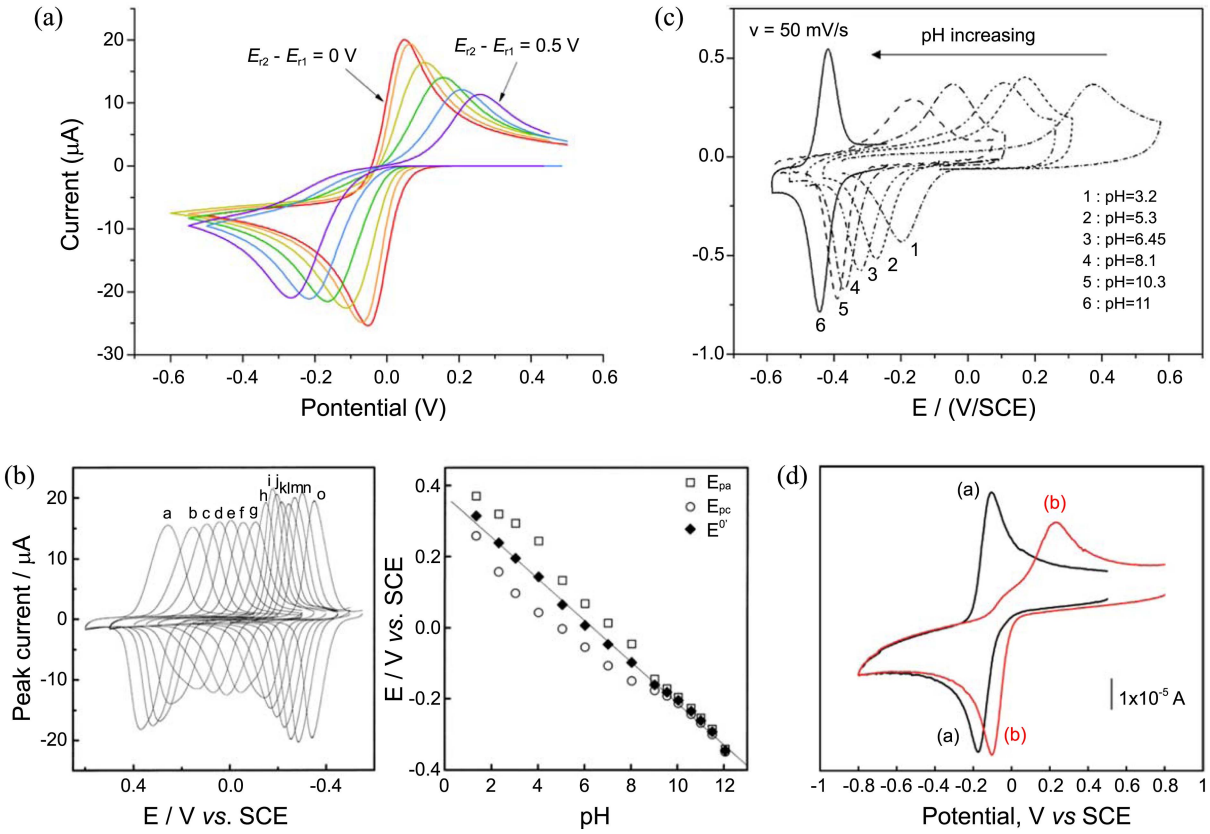

Figure 6. (a) Simulated cyclic voltammograms for a general two-electron redox reaction. $k_1 = k_2 = 0.005$ cm/s. $E_{app} = 0$ V. $E_{r2} - E_{r1} = 0$, 0.1, 0.2, 0.3, 0.4, 0.5 V (from red to purple). (b) (left) Cyclic voltammograms of hydroquinone SAMs at various pH values from 1.3 to 12.1. (right) Plot of cathodic and anodic peak potentials and midpoint potentials *versus* pH. Reproduced from ref. 27. with permission of the PCCP Owner Societies. (c) Cyclic voltammograms of ubiquinone-incorporated monolayer at various pH values from 3.2 to 11. Reproduced with permission from ref. 28. © 2001 American Chemical Society. (d) Cyclic voltammogram of 1,4-benzoquinone in (black) unbuffered and (red) buffered pH 7.2 aqueous solution. Reproduced with permission from ref. 19. © 2007 American Chemical Society.

electron redox peak appears, unlike in aprotic media. The equation below shows the quantitative relationship between semiquinone stability and E_{ri} values.[26]

$$\log\frac{[Q_{sem}]^2}{[Q_{ox}][Q_{red}]} = -\frac{F}{RT}(E_{r2}-E_{r1})$$

The degree of potential inversion, or the value of $E_{r2} - E_{r1}$, also critically affects the overall electrochemical reaction rate. Rate constant k_{app} is

$$k_{app} = k_{ri}\exp\left\{-\frac{F}{4RT}(E_{r2}-E_{r1})\right\}$$

with $k_{ri} = k_{r1}$ or k_{r2} depending on which is the rate-determining step. Therefore the larger the value of $E_{r2} - E_{r1}$, the smaller the apparent rate is. Simulated voltammograms of a general two-electron redox reaction show slower kinetics for larger values of potential inversion (Figure 6(a)), when all other parameters equal. This is peculiar in some way because a large degree of potential inversion means the driving force for the following second electron transfer is large; nonetheless large potential inversion results in a decrease of the overall rate of redox interconversion and a wide peak-to-peak separation in the cyclic voltammogram. Though small k_{app} or wide peak-to-peak separation is often associated simply with a slow rate of electron transfer (small value of k_{r1} or k_{r2}), it may result from an increase of $E_{r2} - E_{r1}$. For quinones, it can be brought about by pH shift as discussed earlier and experimental examples are shown in figure 6B and 6C. The smaller peak-to-peak separation in unbuffered solutions with $[H^+] << [Q]$ is also due to smaller $E_{r2} - E_{r1}$ for the reaction $Q \rightleftharpoons Q^{2-}$ than $Q \rightleftharpoons QH_2$ (Figure 6(d)).

Mechanism Studies of the Square Scheme. Analysis of the square scheme provides further details about the mechanism, as presented in the complete analytical description given by Laviron.[21,29] He derived expressions for E_{r1}, E_{r2}, k_{app} and other parameters of interest, and applied his theory to interpret the Tafel plot data of 1,4-benzoquinone/hydroquinone couple obtained at a Pt electrode at pH 0-7, from which a good agreement was found. Adopting literature values for some of the E_i and pK_{ai}'s, he determined the unknown pK_{ai} and rate constant k_i's in the square scheme, though an unusually large value of k_2 raised suspicion of adsorption effect. The sequence of electron and proton transfers at different pH values was also suggested. For example, at pH 7 the sequence was $Q - Q^{\bullet-} - QH^{\bullet} - QH^{-} - QH_2$, or eHeH for reduction and HeHe for oxidation.

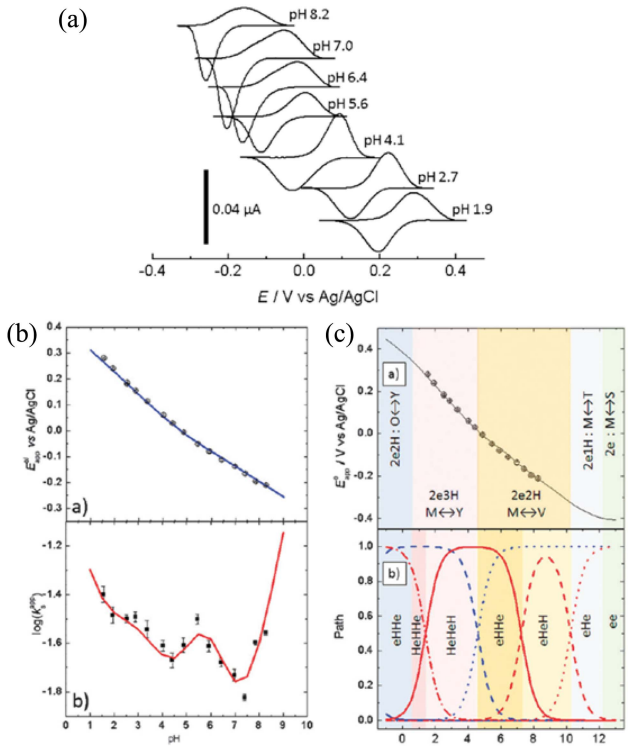

Figure 7. Mechanistic investigation of aminobenzoquinone monolayers. (a) Baseline corrected cyclic voltammograms at various pH. (b) Variation of E_{app} and k_{app} *versus* pH. (c) Reaction sequence at different pH values. Reproduced from ref. 32 with permission of the PCCP Owner Societies.

Application of Laviron's framework followed, *i.e.*, E_i, pK_{ai} and k_i values that constitute the square scheme (Figure 4) were determined by fitting the calculated E_{app} and k_{app} values to experimental data in a wide pH range, along with literature values for some of the E_i and pK_{ai} values. In particular, self-assembled monolayers provided a good platform because k_{app} can be extracted easily with an established protocol,[30] and non-ideal adsorption and interaction with electrode is minimized. It was generally found that pK_a values of $QH^{\bullet}$ and QH_2 tend to increase when quinone is immobilized on electrode surface.[31] With benzoquinone monolayers formed from Michael addition of amine to quinone, an extended 12-membered scheme with an additional protonation state was presented (Figure 7).[32] Ubiquinone could be immobilized on electrode surfaces with its hydrophobic side chain, and neat interpretation with the square scheme was given.[28,33] Instead of extracting k_{app}, some exploited digital simulation software to directly simulate the voltammetric response of water-soluble anthraquinones.[34]

Although the level of detail that quinone/hydroquinone redox reaction can be understood is remarkable, there are limitations in applying Laviron's idealized theoretical framework of the square scheme. Generally there are too many parameters to be determined, and as some authors of the previously mentioned works also acknowledged, a particular set of parameters may not be the only one that fits the experimental data. Moreover, the several assumptions involved in formulating the square scheme indicate that even if a unique set of parameters were obtained as the solution, it is uncertain whether they have true physical meaning. Most importantly, in the classical square scheme analysis, it is assumed that only stepwise pathways are followed, *i.e.* electrons and protons are transferred individually in kinetically distinct steps. However, there are increasing reports of concerted transfer of electron and proton,[8,35,36] and k_{app} has been modified to take the concerted pathway into account.[37] Concerted pathway is more likely to step in when pK_a values of oxidized and reduced states are wide apart, as this retards the stepwise pathway at intermediate pH. It was recently shown that homogeneous quinone PCET is a complicated mix of concerted and stepwise pathways.[38]

In addition, it is assumed that protonation/deprotonation equilibria are always maintained. It is a reasonable assumption in buffered aqueous solutions, but caution has to be taken when pK_a values of the oxidized and reduced forms are wide apart.[37] A recent paper suggested that proton transfer becomes faster at nanoporous electrodes based on electrochemical experiments, implying that protonation and deprotonation reactions may not be infinitely fast.[39] Also, pro-

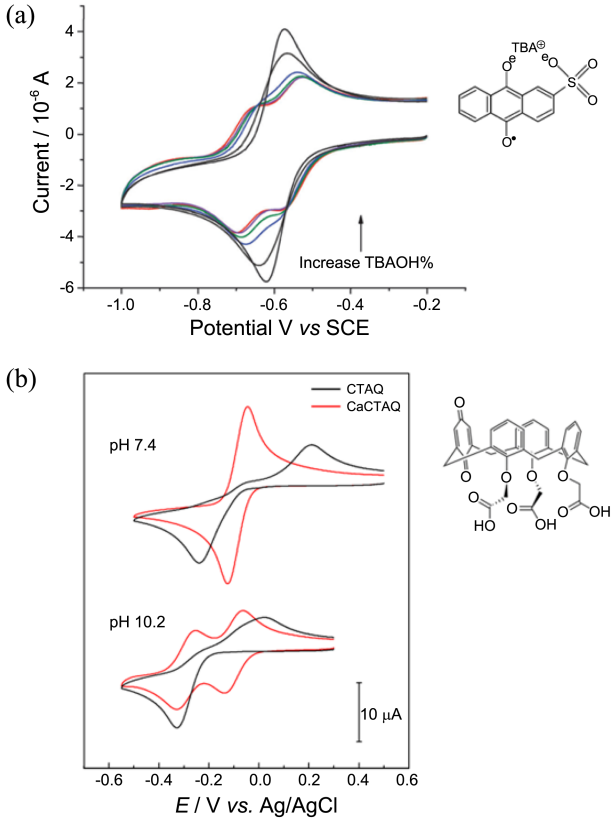

Figure 8. Cyclic voltammograms of anthraquinone-2-sulfonate in ([TMAOH]+[TBAOH]) = 0.1 M (TMA^+ = tetramethylammonium, TBA^+ = tetrabutylammonium). The proportion of TBAOH increases from (black) 0% to (red) 100%. Reproduced with permission from ref. 42. © 2011 Royal Society of Chemistry. (b) Cyclic voltammograms of calix[4]arene-triacid-monoquinone (CTAQ) (red) with and (black) without Ca^{2+} in buffered aqueous solutions. Reproduced with permission from ref. 43. © 2013 American Chemical Society.

ton transfer may become slow when quinone is immobilized on the surface of electrode and steric or hydrophobic barrier is created around the quinone.[40] Readers further interested in mechanism analysis may find an extensive review on this topic helpful.[8]

Semiquinone Radical Stabilization by Cations. Due to the strong hydrogen bonding ability of water that stabilizes Q^{2-} far more than $Q^{\bullet-}$, it was thought that it is impossible to create a situation where $E_{r2} < E_{r1}$ in aqueous solutions and observe separate two one-electron peaks as in nonaqueous solutions. However, it was revealed that in some cases cations can stabilize $Q^{\bullet-}$ selectively in aqueous solutions. Anthraquinone sulfonate in 0.1 M hydroxide solutions showed "peak splitting" when bulky tetrabutylammonium cation (TBA^+) was employed as the supporting electrolyte cation and was proposed to ion-pair with $Q^{\bullet-}$, stabilizing it (Figure 8(a)).[41,42] Because of the high pH, no protonation was involved. The midpoint potential was little changed, indicating that the thermodynamics of the overall reaction $Q \rightleftarrows Q_{red}$ was little affected by the ion pairing effect. The enhanced stability of Q_{sem} was confirmed from the lowered rate of catalytic oxygen reduction, which is mediated by Q_{sem}.[42] However, the cause of selective stabilization of Q_{sem} over Q_{red} by ion pairing was not given clearly.

In a more recent example, peak splitting was even observed at lower pH and in the presence of protonation.[43] A quinone-containing ionophoric molecule (Figure 8(b)) was devised to capture a metal ion in the vicinity of the quinone moiety, influencing its voltammetric response. When Ca^{2+} cation was captured, the semiquinone radical was greatly stabilized and a wide peak splitting occurred at pH 10.2, the corresponding reactions being $Q \rightleftarrows Q^{\bullet-}$ and $Q^{\bullet-} \rightleftarrows QH^-$. At neutral pH, the broad peak-to-peak separation of ~400 mV was reduced to ~80 mV. This was caused by a dramatic decrease in $E_{r2} - E_{r1}$, *i.e.* semiquinone stabilization. As a proof, the stable semiquinone radical was observed with EPR and spectroelectrochemistry. A study that shows semiquinone stabilization of pyrroloquinoline quinone (PQQ) cofactor in soluble glucose dehydrogenase by Ca^{2+} cation implies the biological significance of this[44].

It is worth making a brief note about the semiquinone radical Q_{sem}, of which stability and properties are of considerable interest because semiquinone radical contributes to reactive oxygen species generation. Q_{sem} stability is determined by $E_{r2} - E_{r1}$, as noted previously, and Q_{sem} stability of various quinone compounds has been tabulated.[26] Q_{sem} can react with O_2 easily to generate the superoxide radical $O_2^{\bullet-}$, because there is no spin restriction unlike most other reactions of organic compounds with O_2.[45] Thanks to fast disproportionation and comproportionation, Q_{sem} exists when Q_{ox} and Q_{red} are present together, even if no redox peak for semiquinone radical is seen in the cyclic voltammogram. It is deemed that the primary mechanism of highly toxic superoxide generation *via* quinone compounds involves the semiquinone radical.[25,46] Autoxidation of hydroquinones by O_2 is known to be catalyzed by Q_{ox}, because Q_{ox} can produce Q_{sem} by reacting with hydroquinone, Q_{red}. In the Q cycle of mitochondria, it is very difficult to observe the semiquinone radical at the Q_o site, which probably acts to suppress superoxide generation.[5] Shift of E_{r1} and E_{r2} by metal cation complexation affects semiquinone stability and several accounts show that metal ion can increase the autoxidation rate of catechols.[47,48] It is still of considerable interest to understand the influence of various factors on semiquinone radical stability and electronic structure calculations have been performed.[49,50] Band assignments of vibrational peaks along with *ab initio* calculation helped elucidate electronic structure of semiquinones as well.[51]

Application of Quinone Electrochemistry

In the previous section, general description of the redox mechanism of quinone was given. The importance of the

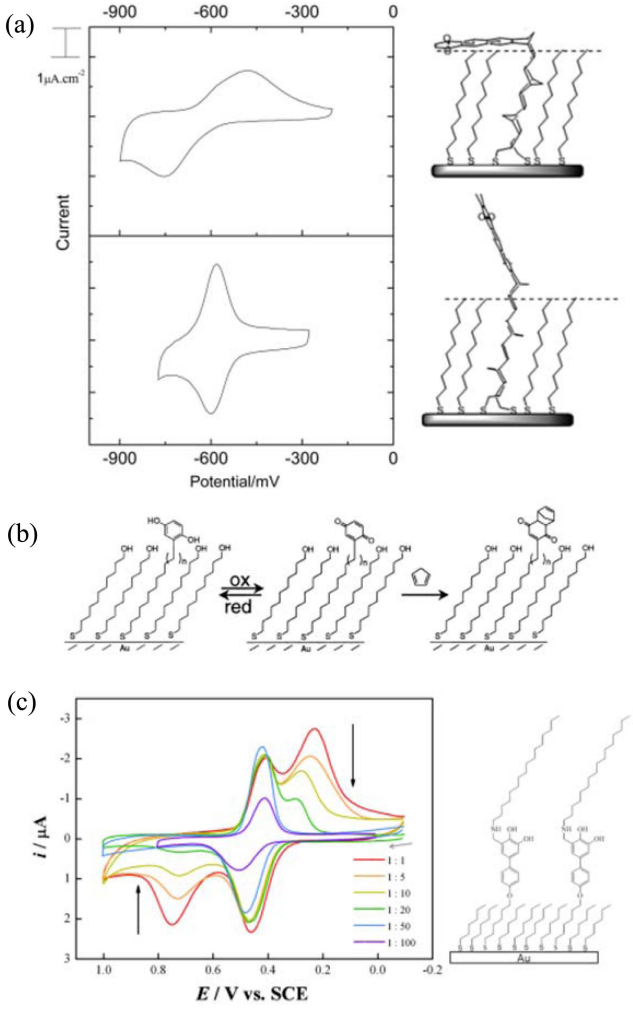

Figure 9. (a) Cyclic voltammograms of different anthraquinone-norbornyl SAMs. Reproduced with permission from ref. 53. © 2012 American Chemical Society. (b) Scheme for probing the kinetics of interfacial Diels-Alder reaction. Reproduced with permission from ref. 54. © 2002 American Chemical Society. (c) Cyclic voltammograms of quinone SAMs with long alkyl chains at different dilution ratio. With higher dilution, the peaks with large peak-to-peak separation decrease. Reproduced with permission from ref. 55. © 2014 Elsevier.

concepts of $Q^{\bullet-}/Q^{2-}$ stabilization and E_{r1}, E_{r2} values were emphasized. It was also shown how electrochemical studies have been conducted to determine the redox mechanism of quinone/hydroquinone, and semiquinone radical stability was discussed. In this section, examples of utilizing quinone redox reaction in various fields of chemistry will be presented. Firstly, quinones can be used as molecular tools for studies in the field of physical chemistry. Secondly, the rapid and stable redox cycling of quinones allows them to be used as versatile electron mediator. Thirdly, the ability of quinones to store and release electrons and protons can be used in organic energy conversion devices. Quinone can be in solution phase or immobilized at the electrode surface by SAM, electrografting or polymerization. As it is impossible to be comprehensible with such a broad scope, we have tried to provide some interesting and representative examples. Readers may also refer to a recent review on the various bio-related applications of quinones.[52]

Molecular Tool for Study on Charge Transfer Kinetics. Quinone tethered to electrode surface can probe the solution environment around the quinone, near the electrode. Darwish *et al.* created novel quinone SAMs that fixed anthraquinone moieties at a set distance and orientation on the electrode by employing rigid norbornylogous linkers (Figure 9(a)).[53] They incorporated diluent molecules having different length and terminal groups, namely –OH or $–CH_3$. The mixed SAMs showed decrease of k_{app} and slight negative shift of E_{app} when the quinone was placed near (< 2.1 Å) the surface of the diluent layer. This was explained by the presence of a thin low-water density layer that was recently revealed to exist at the surface of such diluent layer. The more hydrophobic terminal group $–CH_3$ showed larger reduction in the k_{app}, but when the quinone was far enough from the diluent layer, terminal group had little effect. Mrksich's group utilized the fact that quinone can undergo Diels-Alder reaction with dienes to become electroinactive to measure the rates of Diels-Alder reaction at the SAM-solution interface (Figure 9(b)).[54] The quinone was buried inside the monolayer or exposed to the solution, and each showed different rate for the interfacial Diels-Alder reaction as probed by cyclic voltammetry. Kim *et al.* observed unusual electrochemical response when *ortho*- and *para*-quinone SAMs were buried under long alkyl chains (Figure 9(c)). It was proposed that strong local hydrogen bonding interaction could have given rise to a large value of $E_{r2} - E_{r1}$.[55]

Abhayawardhana *et al.* carried out detailed investigation of amino-anthraquinone monolayer.[56] Impedance analysis implied proton penetration into the monolayer driven by electrode potential, and the origin of very large reorganization energy was attributed to the breaking of intramolecular hydrogen bonding upon redox state change. Chung *et al.* studied proton transfer across organic/aqueous liquid-liquid interface with hydrophobic quinone dissolved in the organic phase.[57] Henstridge *et al.* showed that anthraquinone peak shift may be used to estimate local pH change near the electrode during oxygen reduction at the electrode, which correctly gave two as the number of protons transferred to

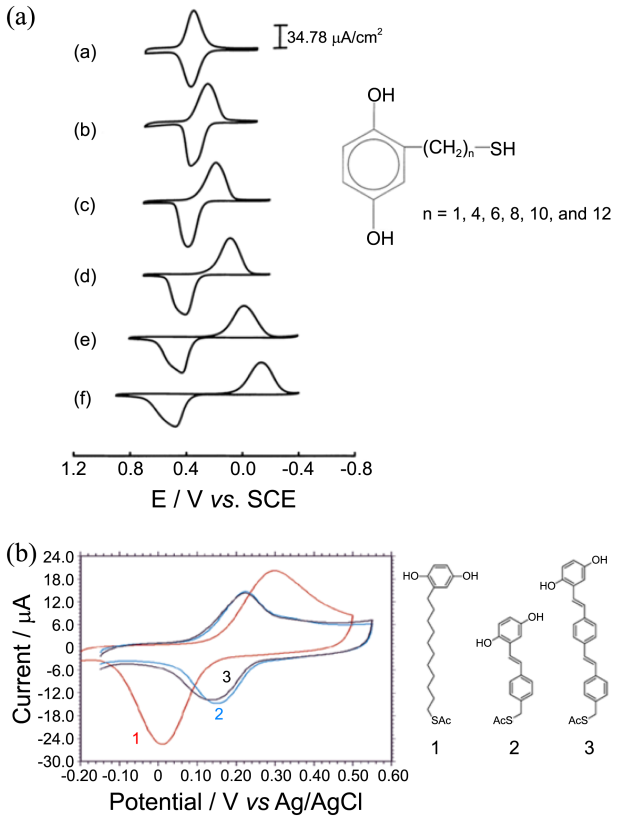

Figure 10. (a) Cyclic voltammograms of quinone SAMs having different linker lengths (linker length increases from a→f). Reproduced with permission from ref. 27. © 2001 American Chemical Society. (b) Cyclic voltammograms of quinone SAMs with different linkers. Reproduced with permission from ref. 60. © 2007 American Chemical Society.

oxygen.[58] Quinone electrochemistry at nanoporous electrodes suggested a new rate enhancement mechanism at nanoporous electrodes.[59] Electrochemical rate enhancement at nanoporous electrodes is often attributed to increased rate of electron transfer from more frequent collision with the electrode, termed confinement effect. By investigating the reaction of quinones, both electron transfer and proton transfer rates were found to increase at nanoporous electrodes.

Quinone-terminated SAMs with different linkers have been studied to reveal the influence of linkers on the interfacial electron transfer rate. Hong *et al.* showed that k_{app} for quinone-terminated alkyl SAMs decreased exponentially with the length of the alkyl linker, in good agreement with expectation from electron tunneling theory and the results of other redox-active SAMs (Figure 10(a)). Trammel *et al.* created quinone SAMs with fully conjugated oligo (phenylene vinylene) linker, which showed enhanced electron transfer rate (Figure 10(b)) compared to simple alkyl linker.[60] Interestingly, for the fully conjugated linkers, rate constant was independent of linker length. They also synthesized linkers containing single, double and triple bonds, and found that rate constant was the largest for double bond and smallest for single bond.[31,61] Another intriguing aspect of these studies is that at high pH where hydroquinone is deprotonated, rate

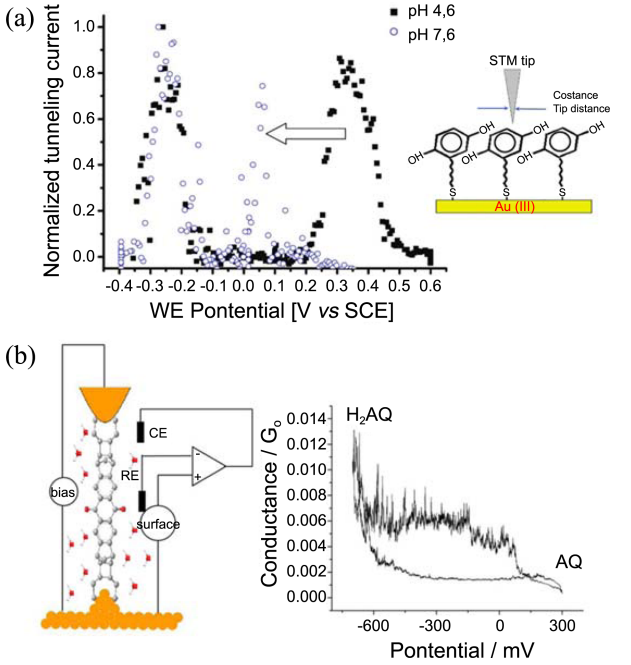

Figure 11. (a) EC-STM of quinone SAM. Tunneling current at different substrate potentials at constant bias voltage and constant tip distance. Reproduced with permission from ref. 65. © 2010 American Chemical Society. (b) Conductance of anthraquinone-bridged junctions. Hydroquinone form shows larger conductance than quinone form. Reproduced with permission from ref. 68. © 2012 American Chemical Society.

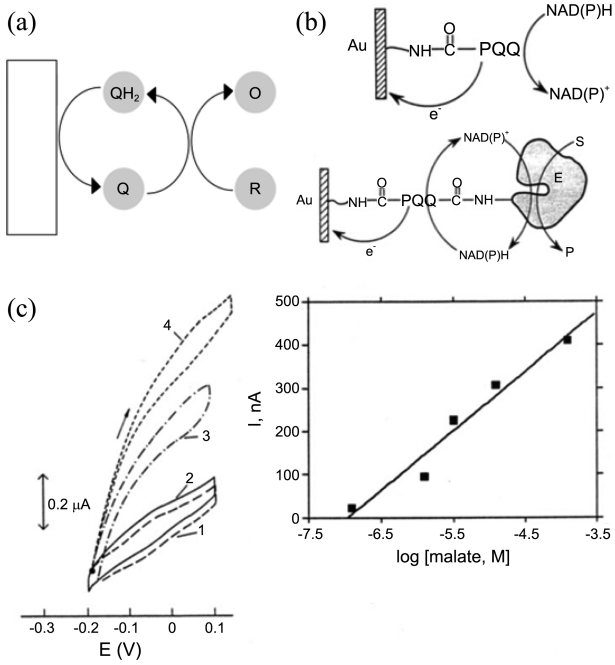

Figure 12. (a) Scheme for amperometric sensing of analyte with quinone as electron mediator. (b) Scheme for amperometric sensing of (top) NADH with PQQ and (bottom) enzyme substrate with NADH/PQQ. (c) Amperometric sensing of malate with the scheme in B. Reproduced with permission from ref. 75. © 1994 American Chemical Society.

constant tends to be independent of linker length.[62,63] Razzaq *et al.* showed that gold nanoparticles sandwiched between the electrode and the quinone layer resulted in rate enhancement.[64]

Direct electron passage from metal substrate to tip *via* molecular bridge can be studied with STM. Electrochemical scanning tunneling microscopy (EC-STM) study of quinones by Petrangolini *et al.* showed interesting results[65-67] (Figure 11(a)). They measured the current through the junction formed between a gold substrate covered with SAM and a gold tip. For such a setup, the tunneling current tends to be enhanced when substrate potential is near the redox potential of the molecule; this phenomenon is called electrolyte gating effect. Remarkably, the tunneling current of hydroquinone-modified junction was found to be enhanced at two different substrate potentials that roughly correspond to the E_{r1} and E_{r2} values of the quinone, and these substrate potential values even mirrored the pH-dependence of E_{r1} and E_{r2}. However, a single redox peak is seen in cyclic voltammograms because electron transfer corresponding to E_{r1} and E_{r2} occur sequentially, *i.e.* second electron transfer can only occur after the first electron transfer. These results were interpreted by regarding E_{r1} and E_{r2} to be different redox levels that can individually contribute to enhancing electron transport through the molecule, which is unique to the EC-STM configuration.[65] Also, when bias voltage (*i.e.* tip-substrate potential difference) was larger than $E_{r2} - E_{r1}$, a region of double enhancement was found, which was thought to be due to the simultaneous participation of both redox levels in tunneling current enhancement.[66] In addition, using different linkers, the presence of a water gap between the quinone and the tip was highlighted.[67] Another interesting study showed that anthraquinone redox state, switched between quinone and hydroquinone by electrochemical gating, affected the conductance of the molecular junction (Figure 11(b)).[68] The cross-conjugated quinone form showed smaller conductance than the hydroquinone form.

Versatile Electron Mediator. The redox of quinone/hydroquinone can provide electronic connection between the electrode and components in the solution. When analyte can induce quinone redox, quinone can be used as the signal transduction element in electrochemical sensors. First, direct electrocatalytic reduction/oxidation of analyte can result in amperometric sensing scheme (Figure 12(a)), in which analyte concentration is known from the amplitude of current. Electrocatalytic oxidation of NADH by quinone is a well-known example,[69-71] and Ca^{2+} ion addition to PQQ-modified electrode was found to increase the amplitude of the electrocatalytic current.[72] Ascorbic acid,[71] hemoglobin[73] and atrazine[74] detection through this scheme have also been reported. To expand the analyte range, quinone layer may be linked to enzymes to mediate electron transfer between the electrode and the enzyme.[75-77] For example, various NADH-dependent oxidases can be linked to the enzyme *via* PQQ to detect the specific substrate of the enzyme (Figure 12(b)).

In another sensing scheme, surface-immobilized quinones reports molecular recognition event nearby. Electrode is

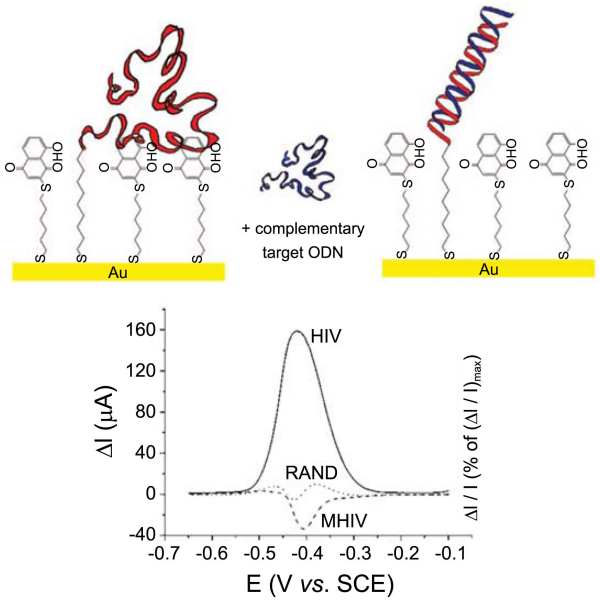

Figure 13. Peak current difference from square wave voltammetry (SWV) for (HIV) complementary, (RAND) random, and (MHIV) single-mismatch DNA strands. DNA hybridization increases the SWV current by removing the steric hindrance over the quinone layer. Reproduced with permission from ref. 79. © 2008 American Chemical Society.

covered with a quinone layer along with probe molecules, and change in steric bulk at the interface caused by molecular recognition alters the amplitude of current from pulse voltammetry. Thanks to such sensitivity of quinone electrochemistry to local chemical environment, no solution-phase

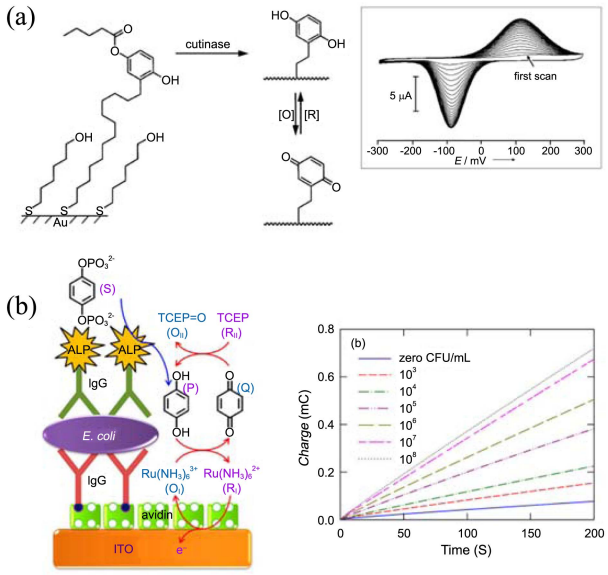

Figure 14. (a) Cutinase activity can be detected from the increase in the cyclic voltammetric peak for quinone/hydroquinone. Reproduced with permission from ref. 82. © 2003 Wiley. (b) *E. coli* detection with electrochemical ELISA using quinones in signal transduction. Charge passed *vs.* time for different concentrations of *E. coli*. Reproduced with permission from ref. 83. © 2013 American Chemical Society.

redox probe for signal transduction is needed. Pham and Piro conducted extensive work on electropolymerized polymeric quinone layers that show stable electrochemical activity and easy functionalization for attaching probe biomolecules.[78] Better sensitivity was achieved with quinone SAM rather than electropolymerized polymeric quinone layer (Figure 13).[79] Mechanistic investigation of these hydroxynaphthoquinone SAMs showed that k_{app} was sensitive to pH at

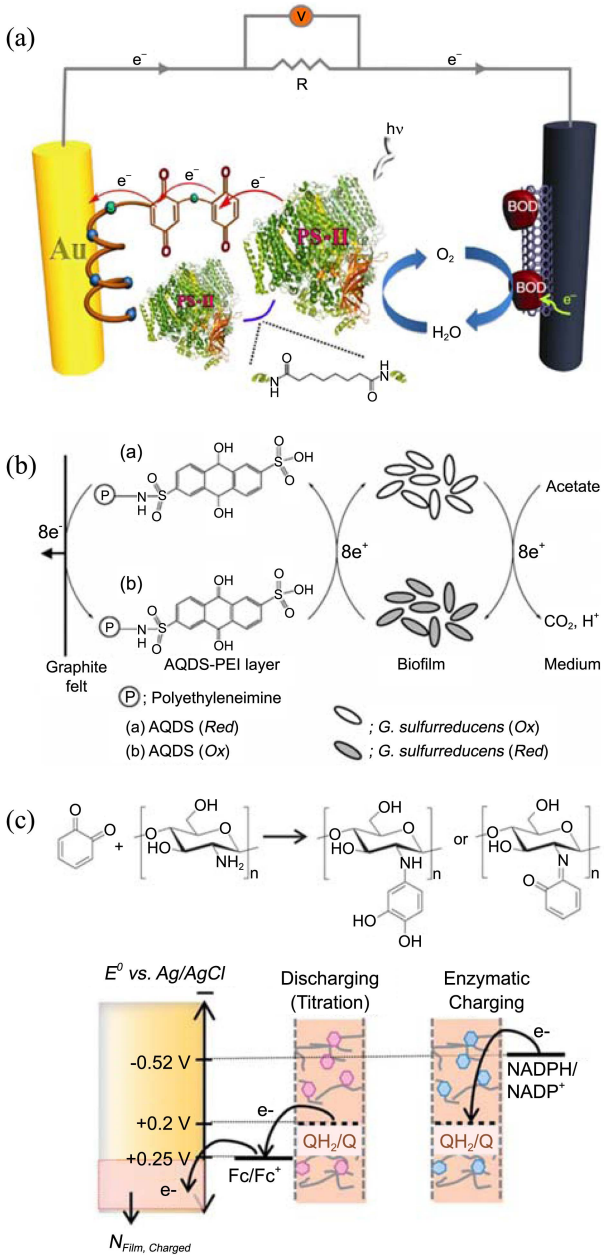

Figure 15. (a) Scheme of photo-bioelectrochemical water splitting cell. Polymeric quinone links photosystem II to gold anode. Reproduced with permission from ref. 84. © 2012 Nature Publishing Group. (b) Microbial fuel cell using anthraquinone-tethered polyethyleneimine (PEI) as electron mediator between the electrode and biofilm. Reproduced with permission from ref. 86. © 2008 Royal Society of Chemistry. (c) Chitosan-quinone film as biological redox capacitor. Reproduced with permission from ref. 89. © 2013 Royal Society of Chemistry.

around pH 7-9.[80] He *et al.* reported a similar example that probed specific saccharide-protein interaction.[81] Pulse voltammetry signal decreased when the protein that had affinity for the saccharide on the electrode was added into the solution, while other proteins had little effect.

A useful feature of quinones is the fact that quinone can be switched from an electrochemically inactive form to an active form. The enzyme cutinase can cleave the ester bond of a protected, electroinactive hydroxyphenyl ester to give an electroactive hydroquinone (Figure 14(a)). Its electrochemical signal indicates the enzyme's activity, so that quinone acts to transduce biological activity to electric signal.[82] It is also possible to increase the sensitivity of amperometric sensing by signal amplification with the redox cycling of freely diffusing solution phase quinone in enzyme-linked immunosorbent assay (ELISA) (Figure 14(b)).[83] The quinone is in the electroinactive hydroquinone diphosphate form at first. The enzyme alkaline phosphatase, linked to the secondary antibody, cleaves the phosphate away to produce electroactive hydroquinone, which subsequently undergoes redox cycling for the amplification of the electrochemical signal.

As already demonstrated, quinones have good potential for connecting biological elements to electrodes electronically by electron mediation. Recently polymeric quinone was used to electrically connect photosystem II to the electrode, which functioned as the anode of a water splitting photo-bioelectrochemical cell (Figure 15(a)).[84] Quinone-modified electrodes were also used for efficient electron exchange with bacterial cells and applied to sensing toxic substances metabolized by bacteria[85] as well as increasing power output of microbial fuel cells[86-88] (Figure 15(b)). Quinone-functionalized chitosan electrodes could be used as a biological redox capacitor that can exchange electrons with biological components in solution, and later convert the amount of charge stored into electronic signal (Figure 15(c)).[89] The film can exchange electrons with solution phase biological components (*e.g.* enzymes) that have difficulty exchanging electrons with the electrode directly. The charge thus stored in the film can be transferred to the electrode and converted to electric signal with added soluble redox species such as ferrocene dimethanol. Interestingly, the chitosan-immobilized quinones were electronically non-conducting, thus allowing it to act as a capacitor.

Charge Storage in Energy Conversion Devices. Quinone/hydroquinone interconversion is equivalent to storing and releasing electrons, which may be applied to green energy conversion technology. Currently it is of great interest to fabricate electrodes from organic materials as they are cheap, lightweight, abundant and degradable. Among others, conjugated carbonyl compounds including quinones are receiving considerable interest.[90] There has been interest in using quinones in batteries for a long time.[91-93] Recently, poly(vinylanthraquinone) polymer immersed in 30 wt % NaOH or KOH solutions was found to exhibit a capacity of 123 mWh/g and stability for over 500 cycles as a rechargeable air battery (Figure 16(a)).[94] The redox current increased dramatically going from neutral to basic pH, and this was explained by better electrolyte permeation in basic pH due to the swelling of polymer chains from charge repulsion between negative Q^{2-}. Quinones were also applied to supercapacitors.[95-97] Supercapacitor capacitance was greatly increased by simply adding hydroquinone into the acid electrolyte (Figure 16(b)),[96] and the capacitance increase was attributed to the quinone redox reaction. Interestingly, quinone redox reaction at the anode caused hydrogen electrosorption to occur at the cathode by holding the anode voltage at a nearly constant value and consequently bringing the cathode potential to large enough values that can induce hydrogen electrosorption (see figure). It was proposed that the overall capacitance is limited by this cathode reaction.[98] Incorporation of quinone into polyvinylalcohol gels was also attempted and similar results were observed.[97]

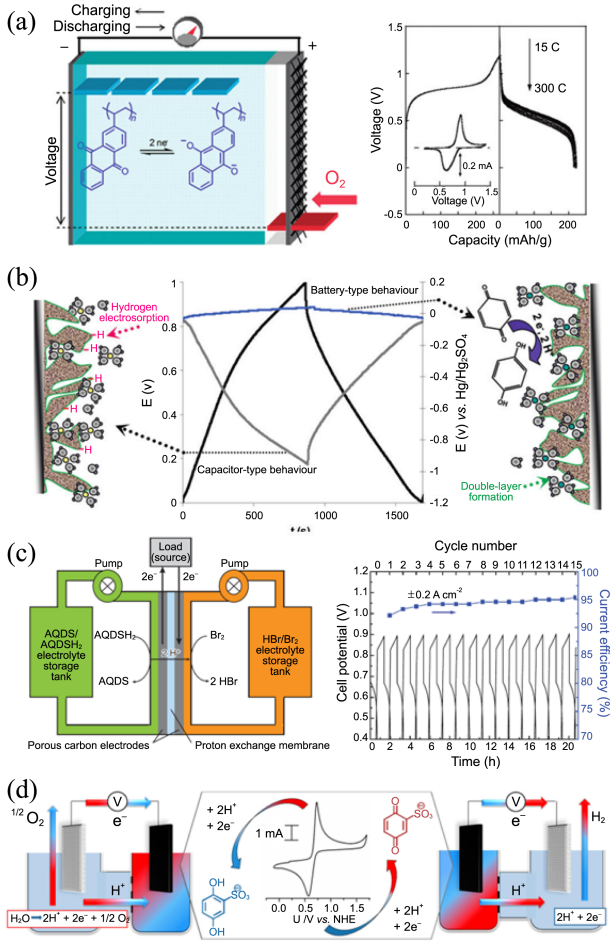

Figure 16. (a) Poly(vinylanthraquinone)/air battery. The charging and discharging curves at various rates and the cyclic voltammogram. Reproduced with permission from ref. 94. © 2011 American Chemical Society. (b) Supercapacitor with quinone-containing electrolyte. Galvanostatic cycling showing (black) cell voltage, (blue) anode potential and (grey) cathode potential variation. Reproduced with permission from ref. 98. © 2011 American Chemical Society. (c) Redox flow battery with Q/QH_2 and Br_2/Br^- and its cycling performance. Reproduced with permission from ref. 99. © 2014 Nature Publishing Group. (d) Water electrolysis with quinone as electron coupled proton buffer (ECPB). Reproduced with permission from ref. 100. © 2013 American Chemical Society.

Solution phase quinones are useful as well. Quinone was the active component in the negative electrolyte in an aqueous redox flow battery (Figure 16(c)).[99] Using simple anthraquinone sulfonates coupled to Br_2/Br^-, stable performance and the possibility of improvement through quinone functionalization were demonstrated. Quinone was also used as electron-coupled proton buffer (ECPB) that aided water electrolysis (Figure 16(d)).[100] The water splitting reaction was divided into the reduction and oxidation half reactions, *i.e.* H_2 evolution and O_2 evolution, to reduce the required cell potential for electrolysis of water. The half reactions were paired up with quinone/hydroquinone half reactions. Because quinone/hydroquinone store and release protons along with electrons, solution pH could be maintained during H_2 or O_2 evolution alone. Quinones were also used to replace the I_3^-/I^- redox couple in the electrolyte of dye-sensitized solar cells.[101,102] In this case, quinone acts as an electron mediator rather than an electron storage compound.

Conclusion

In this account, we presented a wide range of studies involving the redox reaction of quinone/hydroquinone and electrochemical methods. First, an overview of the electrochemical behavior of quinone in different solution environments was given to establish a general understanding of quinone redox mechanism. The case of buffered aqueous solution was treated in more detail, as it could be formulated into a neat 9-membered square scheme. The instability of semiquinone radical in aqueous solutions was explained along with the stabilizing effect of cations. Then, in the second part, we showed various applications of quinone redox reaction probed or induced by electrochemical methods. Quinone could provide information about the chemical environment or electron transfer rate at different interfaces, shuttle electrons between different components of a functional system such as sensors, and offer charge storage capacity in energy conversion devices. We hope that this contribution will help more researchers understand and be comfortable with quinone electrochemistry, which may seem quite complicated at first sight. We also expect to see more researchers in various fields exploit the full potential of quinones for their work.

Acknowledgments. This work was supported by the SRC Program (No. 2007-0056334), the Nano Material Technology Development Program (No. 2011-0030268), and Program No. 2012R1A2A1A03011289 which are funded by the National Research Foundation under the Ministry of Science, ICT & Future Planning, Korea and by the IT R&D program of MKE/KEIT (10041596, Development of Core Technology for TFT Free Active Matrix Addressing Color Electronic Paper with Day and Night Usage).

References

1. Moss, G. P.; Smith, P. A. S.; Tavernier, D. *Pure Appl. Chem.* **2009**, *67*, 1307.
2. Chambers, J. Q. *The Chemistry of Quinonoid Compounds*; Patai, S., Ed.; John Wiley & Sons: Ltd., pp 737-791.
3. Chambers, J. Q. *The Chemistry of Quinonoid Compounds*; Patai, S., Rappaport, Z., Eds.; Great Britain: John Wiley & Sons: pp 719-757.
4. Gunner, M. R.; Madeo, J.; Zhu, Z. *J. Bioenerg. Biomembr.* **2008**, *40*, 509.
5. Osyczka, A.; Moser, C. C.; Dutton, P. L. *Trends Biochem. Sci.* **2005**, *30*, 176.
6. Bolton, J. L.; Trush, M. A.; Penning, T. M.; Dryhurst, G.; Monks, T. J. *Chem. Res. Toxicol.* **2000**, *13*, 135.
7. Hillard, E. A.; Abreu, F. C. de, Ferreira, D. C. M.; Jaouen, G.; Goulart, M. O. F.; Amatore, C. *Chem. Commun.* **2008**, 2612.
8. Costentin, C.; Robert, M.; Savéant, J.-M. *Chem. Rev.* **2010**, *110*, PR1.
9. Cabaniss, G. E.; Diamantis, A. A.; Murphy, W. R.; Linton, R. W.; Meyer, T. J. *J. Am. Chem. Soc.* **1985**, *107*, 1845.
10. DuVall, S. H.; McCreery, R. L. *Anal. Chem.* **1999**, *71*, 4594.
11. Forster, R. J.; O'Kelly, J. P. *J. Electroanal. Chem.* **2001**, *498*, 127.
12. Chaudhari, V. R.; Bhat, M. A.; Ingole, P. P.; Haram, S. K. *Electrochem. Commun.* **2009**, *11*, 994.
13. Eggins, B. R.; Chambers, J. Q. *J. Electrochem. Soc.* **1970**, *117*, 186.
14. Gupta, N.; Linschitz, H. *J. Am. Chem. Soc.* **1997**, *119*, 6384.
15. Aguilar-Martinez, M.; Macías-Ruvalcaba, N. A.; Bautista-Martínez, J. A.; Gómez, M.; González, F. J.; González, I. *Curr. Org. Chem.* **2004**, *8*, 1721.
16. Gómez, M.; González, F. J.; González, I. *J. Electroanal. Chem.* **2005**, *578*, 193.
17. Guin, P. S.; Das, S.; Mandal, P. C. *Int. J. Electrochem.* **2011**, *2011*, 1.
18. Hui, Y.; Chng, E. L. K.; Chng, C. Y. L.; Poh, H. L.; Webster, R. D. *J. Am. Chem. Soc.* **2009**, *131*, 1523.
19. Quan, M.; Sanchez, D.; Wasylkiw, M. F.; Smith, D. K. *J. Am. Chem. Soc.* **2007**, *129*, 12847.
20. Shim, Y.-B.; Park, S.-M. *J. Electroanal. Chem.* **1997**, *425*, 201.
21. Laviron, E. *J. Electroanal Chem Interfacial Electrochem.* **1984**, *164*, 213.
22. Eigen, M. *Discuss. Faraday Soc.* **1965**, *39*, 7.
23. Bailey, S. I.; Ritchie, I. M.; Hewgill, F. R. *J. Chem. Soc. Perkin Trans. 2* **1983**, 645.
24. Bailey, S. I.; Ritchie, I. M. *Electrochimica Acta* **1985**, *30*, 3.
25. Song, Y.; Buettner, G. R. *Free Radic. Biol. Med.* **2010**, *49*, 919.
26. Roginsky, V. A.; Pisarenko, L. M.; Bors, W.; Michel, C. *J. Chem. Soc. Perkin Trans. 2* **1999**, 871.
27. Hong, H.-G.; Park, W. *Langmuir* **2001**, *17*, 2485.
28. Lemmer, C.; Bouvet, M.; Meunier-Prest, R. *Phys. Chem. Chem. Phys.* **2011**, *13*, 13327.
29. Laviron, E. *J. Electroanal. Chem. Interfacial Electrochem.* **1983**, *146*, 15.
30. Laviron, E. *J. Electroanal. Chem.* **1979**, *101*, 19.
31. Trammell, S. A.; Lebedev, N. *J. Electroanal. Chem.* **2009**, *632*, 127.
32. Zhang, W.; Burgess, I. J. *Phys. Chem. Chem. Phys.* **2011**, *13*, 2151.
33. Marchal, D.; Boireau, W.; Laval, J. M.; Bourdillon, C.; Moiroux, J. *J. Electroanal. Chem.* **1998**, *451*, 139.
34. Batchelor-McAuley, C.; Li, Q.; Dapin, S. M.; Compton, R. G. *J. Phys. Chem. B* **2010**, *114*, 4094.
35. Costentin, C.; Louault, C.; Robert, M.; Savéant, J.-M. *Proc. Natl. Acad. Sci.* **2009**, *106*, 18143.
36. Medina-Ramos, J.; Oyesanya, O.; Alvarez, J. C. *J. Phys. Chem. C* **2013**, *117*, 902.
37. Anxolabéhère-Mallart, E.; Costentin, C.; Policar, C.; Robert, M.; Savéant, J.-M.; Teillout, A.-L. *Faraday Discuss.* **2010**, *148*, 83.
38. Song, N.; Gagliardi, C. J.; Binstead, R. A.; Zhang, M.-T.; Thorp, H.; Meyer, T. J. *J. Am. Chem. Soc.* **2012**, *134*, 18538.
39. Bae, J. H.; Kim, Y.-R.; Kim, R. S.; Chung, T. D. *Phys. Chem.*

Chem. Phys. **2013**, *15*, 10645.
40. Moncelli, M. R.; Herrero, R.; Becucci, L.; Guidelli, R. *Biochim. Biophys. Acta BBA - Bioenerg.* **1998**, *1364*, 373.
41. Gamage, R. S. K. A.; McQuillan, A. J.; Peake, B. M. *J. Chem. Soc. Faraday Trans.* **1991**, *87*, 3653.
42. Li, Q.; Batchelor-McAuley, C.; Lawrence, N. S.; Hartshorne, R. S.; Compton, R. G. *Chem. Commun.* **2011**, 11426.
43. Kim, Y.-R.; Kim, R. S.; Kang, S. K.; Choi, M. G.; Kim, H. Y.; Cho, D.; Lee, J. Y.; Chang, S.-K.; Chung, T. D. *J. Am. Chem. Soc.* **2013**, *135*, 18957.
44. Sato, A.; Takagi, K.; Kano, K.; Kato, N.; Duine, J.; Ikeda, T. *Biochem. J.* **2001**, *357*, 893.
45. Buchachenko, A. L. *Pure Appl. Chem.* **2000**, *72*, 2243.
46. Roginsky, V.; Barsukova, T. *J. Chem. Soc. Perkin Trans. 2* **2000**, 1575.
47. Lebedev, A. V.; Ivanova, M. V.; Ruuge, E. K. *Arch. Biochem. Biophys.* **2003**, *413*, 191.
48. Lebedev, A. V.; Ivanova, M. V.; Timoshin, A. A.; Ruuge, E. K. *ChemPhysChem* **2007**, *8*, 1863.
49. O'Malley, P. J. *J. Phys. Chem. A* **1998**, *102*, 248.
50. Kaupp, M.; Remenyi, C.; Vaara, J.; Malkina, O. L.; Malkin, V. G. *J. Am. Chem. Soc.* **2002**, *124*, 2709.
51. Zhao, X.; Imahori, H.; Zhan, C.-G.; Sakata, Y.; Iwata, S.; Kitagawa, T. *J. Phys. Chem. A* **1997**, *101*, 622.
52. Ma, W.; Long, Y.-T. *Chem. Soc. Rev.* **2013**, *43*, 30.
53. Darwish, N.; Eggers, P. K.; Ciampi, S.; Tong, Y.; Ye, S.; Paddon-Row, M. N.; Gooding, J. J. *J. Am. Chem. Soc.* **2012**, *134*, 18401.
54. Kwon, Y.; Mrksich, M. *J. Am. Chem. Soc.* **2002**, *124*, 806.
55. Kim, R. S.; Park, W.; Hong, H.; Chung, T. D.; Kim, S. *Electrochem. Commun.* **2014**, *41*, 39.
56. Abhayawardhana, A. D.; Sutherland, T. C. *J. Phys. Chem. C* **2009**, *113*, 4915.
57. Chung, T. D.; Anson, F. C. *Anal. Chem.* **2001**, *73*, 337.
58. Henstridge, M. C.; Wildgoose, G. G.; Compton, R. G. *Langmuir* **2010**, *26*, 1340.
59. Bae, J. H.; Kim, Y.-R.; Kim, R. S.; Chung, T. D. *Phys. Chem. Chem. Phys.* **2013**, *15*, 10645.
60. Trammell, S. A.; Seferos, D. S.; Moore, M.; Lowy, D. A.; Bazan, G. C.; Kushmerick, J. G.; Lebedev, N. *Langmuir* **2007**, *23*, 942.
61. Trammell, S. A.; Moore, M.; Schull, T. L.; Lebedev, N. *J. Electroanal. Chem.* **2009**, *628*, 125.
62. Hong, H.-G.; Park, W. *Bull. Korean Chem. Soc.* **2005**, *26*, 1885.
63. Trammell, S. A.; Lowy, D. A.; Seferos, D. S.; Moore, M.; Bazan, G. C.; Lebedev, N. *J. Electroanal. Chem.* **2007**, *606*, 33.
64. Razzaq, H.; Qureshi, R.; Schiffrin, D. J. *Electrochem. Commun.* **2014**, *39*, 9.
65. Petrangolini, P.; Alessandrini, A.; Berti, L.; Facci, P. *J. Am. Chem. Soc.* **2010**, *132*, 7445.
66. Petrangolini, P.; Alessandrini, A.; Navacchia, M. L.; Capobianco, M. L.; Facci, P. *J. Phys. Chem. C* **2011**, *115*, 19971.
67. Petrangolini, P.; Alessandrini, A.; Facci, P. *J. Phys. Chem. C* **2013**, *117*, 17451.
68. Darwish, N.; Díez-Pérez, I.; Guo, S.; Tao, N.; Gooding, J. J.; Paddon-Row, M. N. *J. Phys. Chem. C* **2012**, *116*, 21093.
69. Tse, D. C.-S.; Kuwana, T. *Anal. Chem.* **1978**, *50*, 1315.
70. Carlson, B. W.; Miller, L. L. *J. Am. Chem. Soc.* **1985**, *107*, 479.
71. Murthy, A. S. N.; Sharma, J. *Talanta* **1998**, *45*, 951.
72. Katz, E.; Lötzbeyer, T.; Schlereth, D. D.; Schuhmann, W.; Schmidt, H.-L. *J. Electroanal. Chem.* **1994**, *373*, 189.
73. Zhang, J.; Seo, K.; Jeon, I. C. *Anal. Bioanal. Chem.* **2003**, *375*, 539.
74. Umezawa, N.; Tsurunari, M.; Kondo, T. *Chem. Lett.* **2009**, *38*, 766.
75. Willner, I.; Riklin, A. *Anal. Chem.* **1994**, *66*, 1535.
76. Bardea, A.; Katz, E.; Bückmann, A. F.; Willner, I. *J. Am. Chem. Soc.* **1997**, *119*, 9114.
77. Willner, I.; Katz, E. *Angew. Chem. Int. Ed.* **2000**, *39*, 1180.
78. Piro, B.; Reisberg, S.; Anquetin, G.; Duc, H.-T.; Pham, M.-C. *Biosensors* **2013**, *3*, 58.
79. March, G.; Noël, V.; Piro, B.; Reisberg, S.; Pham, M.-C. *J. Am. Chem. Soc.* **2008**, *130*, 15752.
80. March, G.; Reisberg, S.; Piro, B.; Pham, M.-C.; Delamar, M.; Noel, V.; Odenthal, K.; Hibbert, D. B.; Gooding, J. J. *J. Electroanal. Chem.* **2008**, *622*, 37.
81. He, X.-P.; Wang, X.-W.; Jin, X.-P.; Zhou, H.; Shi, X.-X.; Chen, G.-R.; Long, Y.-T. *J. Am. Chem. Soc.* **2011**, *133*, 3649.
82. Yeo, W.-S.; Mrksich, M. *Angew. Chem. Int. Ed.* **2003**, *42*, 3121.
83. Akanda, M. R.; Tamilavan, V.; Park, S.; Jo, K.; Hyun, M. H.; Yang, H. *Anal. Chem.* **2013**, *85*, 1631.
84. Yehezkeli, O.; Tel-Vered, R.; Wasserman, J.; Trifonov, A.; Michaeli, D.; Nechushtai, R.; Willner, I. *Nat. Commun.* **2012**, *3*, 742.
85. Aulenta, F.; Ferri, T.; Nicastro, D.; Majone, M.; Papini, M. P. *New Biotechnol.* **2011**, *29*, 126.
86. Adachi, M.; Shimomura, T.; Komatsu, M.; Yakuwa, H.; Miya, A. *Chem. Commun.* **2008**, 2055.
87. Feng, C.; Ma, L.; Li, F.; Mai, H.; Lang, X.; Fan, S. *Biosens. Bioelectron.* **2010**, *25*, 1516.
88. Ahmed, J.; Kim, S. *Bull. Korean Chem. Soc.* **2013**, *34*, 3649.
89. Kim, E.; Leverage, W. T.; Liu, Y.; White, I. M.; Bentley, W. E.; Payne, G. F. *Analyst* **2013**, *139*, 32.
90. Song, Z.; Zhou, H. *Energy Environ. Sci.* **2013**, *6*, 2280.
91. Alt, H.; Binder, H.; Köhling, A.; Sandstede, G. *Electrochimica Acta* **1972**, *17*, 873.
92. Foos, J. S.; Erker, S. M.; Rembetsy, L. M. *J. Electrochem. Soc.* **1986**, *133*, 836.
93. Le Gall, T.; Reiman, K. H.; Grossel, M. C.; Owen, J. R. *J. Power Sources* **2003**, *119-121*, 316.
94. Choi, W.; Harada, D.; Oyaizu, K.; Nishide, H. *J. Am. Chem. Soc.* **2011**, *133*, 19839.
95. Suematsu, S.; Naoi, K. *J. Power Sources* **2001**, *97-98*, 816.
96. Roldán, S.; Blanco, C.; Granda, M.; Menéndez, R.; Santamaría, R. *Angew. Chem. - Int. Ed.* **2011**, *50*, 1699.
97. Yu, H.; Wu, J.; Fan, L.; Lin, Y.; Xu, K.; Tang, Z.; Cheng, C.; Tang, S.; Lin, J.; Huang, M. *et al. J. Power Sources* **2012**, *198*, 402.
98. Roldán, S.; Granda, M.; Menéndez, R.; Santamaría, R.; Blanco, C. *J. Phys. Chem. C* **2011**, *115*, 17606.
99. Huskinson, B.; Marshak, M. P.; Suh, C.; Er, S.; Gerhardt, M. R.; Galvin, C. J.; Chen, X.; Aspuru-Guzik, A.; Gordon, R. G.; Aziz, M. J. *Nature* **2014**, *505*, 195.
100. Rausch, B.; Symes, M. D.; Cronin, L. *J. Am. Chem. Soc.* **2013**, *135*, 13656.
101. Pichot, F.; Gregg, B. A. *J. Phys. Chem. B* **2000**, *104*, 6.
102. Cheng, M.; Yang, X.; Zhang, F.; Zhao, J.; Sun, L. *Angew. Chem. Int. Ed.* **2012**, *51*, 9896.